ANNUAL REVIEWS **Further**

Click here for quick links to Annual Reviews content online, including:

- Other articles in this volume
- Top cited articles
- Top downloaded articles
- Our comprehensive search

Annu. Rev. Biochem. 2008.77:51-76. Downloaded from www.annualreviews.org
by Kanazawa University Medical Library Branch on 09/07/10. For personal use only.

Advances in Single-Molecule Fluorescence Methods for Molecular Biology

Chirlmin Joo,[1] Hamza Balci,[1] Yuji Ishitsuka,[1,2] Chittanon Buranachai,[3] and Taekjip Ha[1,2,3]

[1]Department of Physics, [2]Howard Hughes Medical Institute, and [3]Center for Biophysics and Computational Biology, University of Illinois at Urbana-Champaign, Urbana, Illinois 61801; chirlmin@gmail.com, balci@uiuc.edu, yuji@uiuc.edu, buranach@uiuc.edu, tjha@uiuc.edu

Annu. Rev. Biochem. 2008. 77:51–76

First published online as a Review in Advance on April 15, 2008

The *Annual Review of Biochemistry* is online at biochem.annualreviews.org

This article's doi:
10.1146/annurev.biochem.77.070606.101543

Copyright © 2008 by Annual Reviews.
All rights reserved

0066-4154/08/0707-0051$20.00

Key Words

fluorophore, force spectroscopy, FRET, live cell imaging, polarization, single-particle tracking

Abstract

Ever since their introduction two decades ago, single-molecule (SM) fluorescence methods have matured and branched out to address numerous biological questions, which were inaccessible via ensemble measurements. Among the current arsenal, SM fluorescence techniques have capabilities of probing the dynamic interactions of nucleic acids and proteins via Förster (fluorescence) resonance energy transfer (FRET), tracking single particles over microns of distances, and deciphering the rotational motion of multisubunit systems. In this exciting era of transitioning from in vitro to in vivo and in situ conditions, it is anticipated that SM fluorescence methodology will become a common tool of molecular biology.

Annu. Rev. Biochem. 2008.77:51-76. Downloaded from www.annualreviews.org
by Kanazawa University Medical Library Branch on 09/07/10. For personal use only.

Contents

INTRODUCTION 52
Brief History 52
Technical Advances 52
Fluorophores 53
FRET STUDIES 54
Surface-Tethered Molecules 54
Freely Diffusing Molecules 58
Confined Molecules 59
TRACKING 60
Translocation 61
Rotational Motion 61
TRACKING IN LIVE CELLS 65
Membrane Proteins 65
Cytoplasmic Proteins 66
Other Single Objects 67
MEASUREMENTS UNDER FORCE 67
Optical Tweezers 67
Magnetic Tweezers 69
Laminar Flow 69
FINAL CONSIDERATIONS 69
CONCLUSION 70

INTRODUCTION

Single-molecule (SM) measurement techniques have revolutionized biological inquiries by providing previously unobtainable data on elementary molecular processes. In particular, fluorescence measurements at the SM level have undergone an explosive growth of late, and here we survey recent technological milestones that are making the approach even more poweful.

SM: single molecule

Fluorophore: a molecule that emits fluorescence photons after being excited

TIRF: total internal reflection fluorescence

FRET: Förster (fluorescence) resonance energy transfer

SPT: single-particle tracking

SNR: signal-to-noise ratio

Brief History

Two decades ago, detection of single fluorescent molecules was demonstrated for the first time at liquid helium temperatures by spectrally isolating the signal from a SM embedded among trillions of host crystal molecules (1, 2). Detection of spatially isolated single fluorophores at room temperature paved the way for biological applications (3); however, a major component was still missing: the use of in aqua conditions. This challenge was surpassed with the use of total internal reflection fluorescence (TIRF) microscopy (4), which demonstrated the first biological application and hence set the path for many modern applications. As the techniques matured, more complex biological problems, such as the detection of the enzymatic turnovers of a single cholesterol oxidase, became accessible (5). In the past 10 years, like in many other fields of science, the lure of biological problems dominated the SM-fluorescence field and led to an exponential growth in the number of biological applications (**Figure 1**) and inspired numerous technical advances.

The article is organized as follows. Brief descriptions of technical advances and fluorophores are followed by highlights from representative applications of various techniques such as Förster (fluorescence) resonance energy transfer (FRET) and single-particle tracking (SPT). Then cutting-edge technologies related to live cells and force manipulation are reviewed. The article concludes with short considerations and the future prospects of SM-fluorescence biophysics.

Technical Advances

The low signal-to-noise ratio (SNR) has been the main obstacle for technical developments, as has been the case for many fields in science. Within less than a decade, several developments have made it possible to progress from detecting single fluorophores at cryogenic temperatures to simultaneously identifying multiple fluorophores attached to a biological system in solution at room temperature. First of all, the background signal has effectively been reduced by constraining the illumination to a shallow depth (by using TIRF microscopy) or small volume (by using confocal and two-photon microscopies). Second, fluorophores

Annu. Rev. Biochem. 2008.77:51-76. Downloaded from www.annualreviews.org
by Kanazawa University Medical Library Branch on 09/07/10. For personal use only.

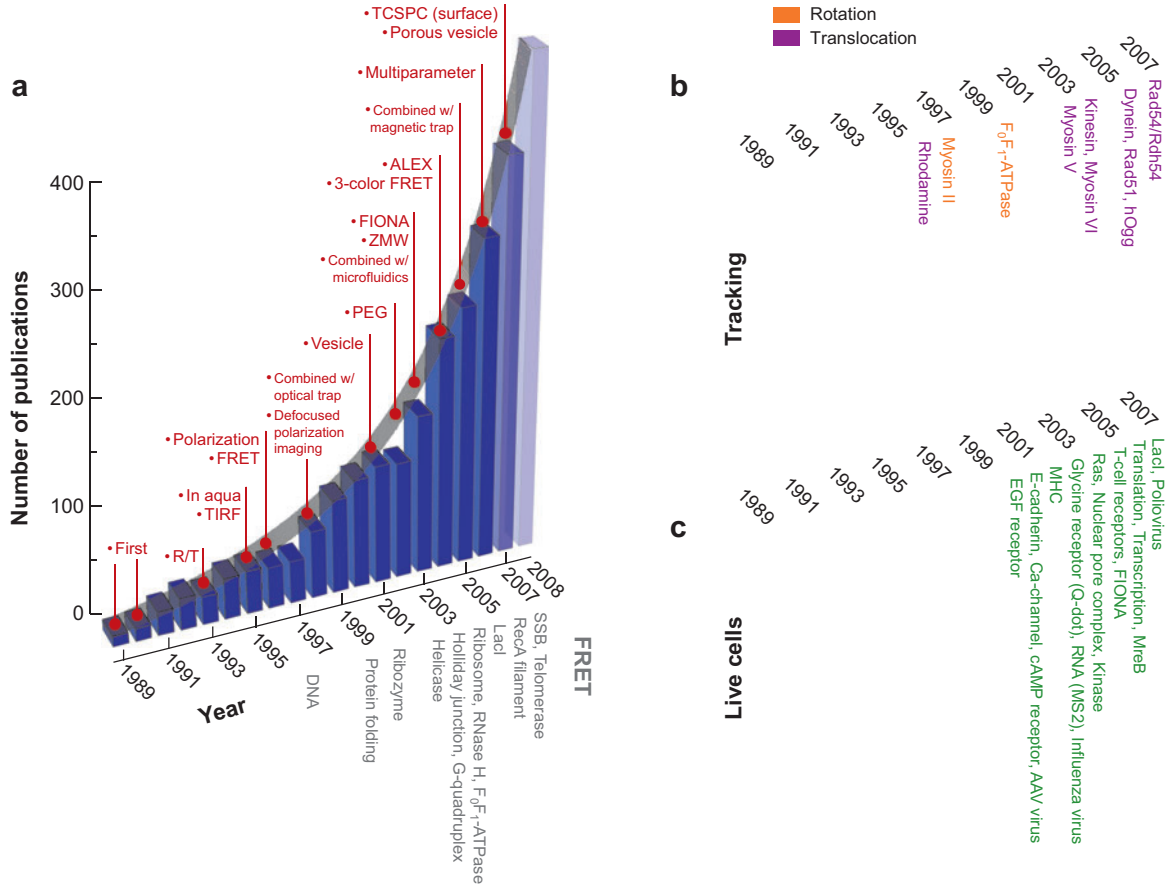

Figure 1

Exponential growth of single-molecule fluorescence work. (*a*) Shown is the number of publications per year, searched in PUBMED with the keyword "single-molecule fluorescence." Major technical advances are marked in *red*. The first studies on important biological systems are listed for FRET (*gray*), tracking translocation (*purple*) and rotation (*orange*), and live cell studies (*green*).

have become brighter and more photostable by carefully tuning the solution conditions. Third, innovations in cooled charge-coupled devices (CCDs) have achieved high quantum yield and zero-dead time together with a submillisecond time resolution. In addition, advances in objective lenses [high numerical aperture (NA), high magnification, and low aberrations] and laser technologies (high-stability, single-mode lasers with various wavelengths) have also been instrumental in achieving the current technical maturity of the field.

Fluorophores

In SM fluorescence spectroscopy, a fluorophore is a storyteller. When attached to a biological molecule, the fluorophore spies on its host and sends back the report in a stream of photons. An ideal SM fluorophore (*a*) has high absorption and fluorescence quantum yield, (*b*) shows steady emission intensity, (*c*) does not perturb the host molecule, and (*d*) stays photoactive over a long time under intense illumination. The majority of in vitro studies currently relies on two major families of fluorophores: cyanine and rhodamine (See

NA: numerical aperture

Annu. Rev. Biochem. 2008.77:51-76. Downloaded from www.annualreviews.org
by Kanazawa University Medical Library Branch on 09/07/10. For personal use only.

FAVORITE FLUOROPHORES

In the cyanine family, the focus is on two of the sulfoindocyanine dyes, Cy3 and Cy5 (8), as they are extensively used either individually (4) or as a FRET pair (9). Both are known for their high absorption coefficient (more than 10^5 M^{-1} cm^{-1}), high photostability, and modest fluorescence quantum yield (10). Other popular dyes include Cy5.5, Cy7, Alexa 555, Alexa 647, and DiI. Other popular dyes in the rhodamine family are tetramethylrhodamine (3, 11), rhodamine 6G, Texas Red, bissulfonerhodamine (12), and some of the Alexa dyes (e.g., 488 and 546). The excitation and the emission spectra of these dyes span across 500–700 nm and are suitable for common lasers and detectors. Several show high quantum yield, low intersystem crossing, and high photostability (13).

sidebar on Favorite Fluorophores). Autofluorescent proteins such as green fluorescent protein (GFP) can bypass the steps of modification and labeling, which is advantageous for live cell experiments. New generations of these fluorophores show a high fluorescence quantum yield with reasonable photostability (6, 7).

MICROSCOPY FOR SM FRET

Similar to many other SM measurements, SM FRET is carried out in a confocal or wide-field microscopy setup. In confocal microscopy, the excitation volume is effectively reduced by tightly focusing the laser beam with a high NA objective lens. The consequent low background signal is ideal for watching both surface-immobilized and freely diffusing SMs. Photon collection is usually achieved with a fast and sensitive point detector, such as an avalanche photodiode, making picosecond time resolution possible.

TIRF microcopy is the most commonly used wide-field detection method for SM applications. An evanescent excitation field, created by refraction through either a prism or a high NA objective lens, allows selective illumination of molecules near the surface (~100 nm) resulting in a low background signal. TIRF microscopy is ideal for monitoring surface-immobilized molecules or tracking lateral movements. Charge-coupled device (CCD) cameras are used for signal detection, enabling simultaneous monitoring of hundreds of SMs with submillisecond time resolution.

FRET STUDIES

FRET between a donor and an acceptor fluorophore takes place, via dipole-dipole interaction, when they are within 10 nm of each other (14). The energy transfer efficiency is given by:

$$E = \frac{1}{1 + (R/R_0)^6},$$

where R is the distance between the pair, and R_0 is the characteristic distance of the pair.

Since the first SM FRET (FRET at the single-molecule level) demonstration on a DNA template (11), SM FRET has been widely used to investigate various biological systems for both intramolecular interactions, such as conformational dynamics of DNA, RNA, and proteins, and intermolecular interactions of proteins with DNA, RNA, and other ligands (**Figure 2**). SM FRET is arguably the most general and adaptable among many SM fluorescence techniques for biology. Here, we discuss the state of the art SM FRET applications by categorizing them into three groups depending on the way the molecules are treated: surface tethered, freely diffusing, and confined molecules. (See sidebar on Microscopy for SM FRET.)

Surface-Tethered Molecules

Many of the relevant biochemical reactions occur in the milliseconds to seconds timescale. Immobilization of molecules (**Figure 2**) allows gathering of long fluorescence time traces, providing the whole history of SM reactions. In this section, a summary of surface immobilization schemes is followed by a review of popular data analysis methods and a description of several advanced techniques, which are based on immobilization schemes.

Nucleic acid studies. Conformational dynamics of DNA (or RNA) can be easily

observed by immobilizing it on a surface coated with biotinylated bovine serum albumin (BSA) via biotin-streptavidin linkage (9, 11). A generic example for this category is the study on the Holliday junction (**Figure 2*a***). A biotin molecule was attached to the end of one of the arms of the Holliday junction such that the other arms labeled with Cy3 (donor) and Cy5 (acceptor) were sufficiently far away from the surface, preventing a possible surface influence on the dynamics of the Holliday junction (15). In this geometry, the two stacking conformations of the junction are differentiated by low and high FRET. The clear anticorrelation between the two fluorescence signals in a time trace (**Figure 2*a***, bottom) directly validated the putative interconversion between the two conformers. A similar approach yielded the observation of folding transitions between three different states of a ribozyme (16).

In some cases, different conformational states may not necessarily possess different FRET values; nevertheless, they may be identified through their distinct lifetimes, called "kinetic fingerprinting" (17). For example, six different states were identified in human telomeric DNA (18), and four different states were distinguished in both branch migration of the Holliday junction (19) and folding and catalysis of the hairpin ribozyme (20). In these studies, the transition rates between conformations were determined by the residence times in particular FRET values; faster transitions (micro- to milliseconds) were typically evaluated by correlation analysis (21, 22).

Protein study on a polymer-coated surface. Studies with proteins require better surface passivation than BSA coating. To this end, surface passivation with linear polyethylene glycol (PEG) was first adopted for SM studies to probe helicase activities (**Figure 2*b***) (23). Nonspecific adsorption of Rep helicase on a PEG-coated surface was 1000 times less than that on a BSA-coated surface, resulting in much better reproduction of bulk activity at the SM level (24).

The PEG-coated surface has been used in many other protein systems interacting with DNA or RNA. The repetitive translocation of the Rep helicase (**Figure 2*b***, left) (25), the unwinding activity of NS3 helicase (**Figure 2*b***, right) (26), the filament dynamics of a RecA recombinase (27), the dynamic binding of a single-stranded (ss) DNA-binding protein (28), and the wrapping dynamics of nucleosomes (29) are several examples of DNA-protein interactions studied on the PEG-coated surface. In addition, the tRNA dynamics while interacting with a ribosome (30), the assembly of a telomerase complex (31), and the annealing activity of a HIV nucleocapsid protein (32) are examples of RNA-protein interactions studied. Another promising approach is surface passivation by lipid bilayers (33).

Protein folding study on an advanced polymer-coated surface. Harsher conditions used for denaturing proteins necessitate more robust passivation; otherwise, surface interaction alters the energy landscape of protein folding pathways. Linear PEG molecules were replaced by branched "star-shaped" PEG to form a dense, cross-linked but thin film (~5 nm) (34). A two-state folding protein, RNAse H, was immobilized via streptavidin-biotin linkage on the star-shaped PEG-coated surface. The protein showed a robust unfolding and refolding behavior even after 50 cycles of switching between native and denaturing buffer conditions. Moreover, the standard Gibbs energy and cooperativity factor of the RNAse H folding were in good agreement with values from tether-free bulk measurements (35).

Model-free data analysis. The observable time trace of a FRET signal is composed of actual fluorescence emissions from different FRET states of the system of interest as well as noise arising from various sources of a statistical, instrumental or photophysical nature. Hence, extracting reliable information from such a complex time trace with multiple

SM FRET: FRET at the single-molecule level

Holliday junction: a four-way junction, which consists of four DNA strands crossing each other and is observed during the recombination process

Correlation analysis: an algorithm that removes high-frequency noise by correlating time-separated data points

PEG: polyethylene glycol

Annu. Rev. Biochem. 2008.77:51-76. Downloaded from www.annualreviews.org
by Kanazawa University Medical Library Branch on 09/07/10. For personal use only.

Annu. Rev. Biochem. 2008.77:51-76. Downloaded from www.annualreviews.org
by Kanazawa University Medical Library Branch on 09/07/10. For personal use only.

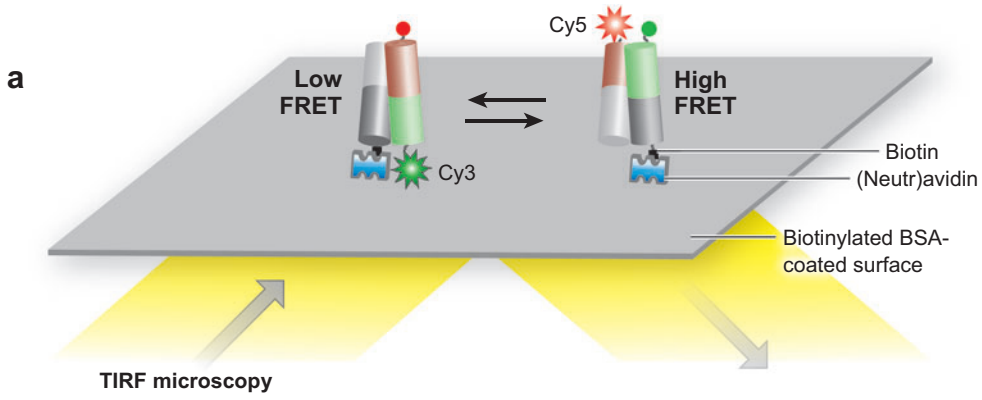

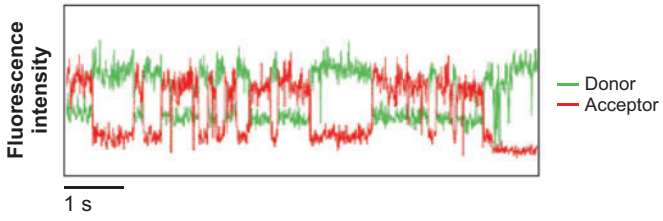

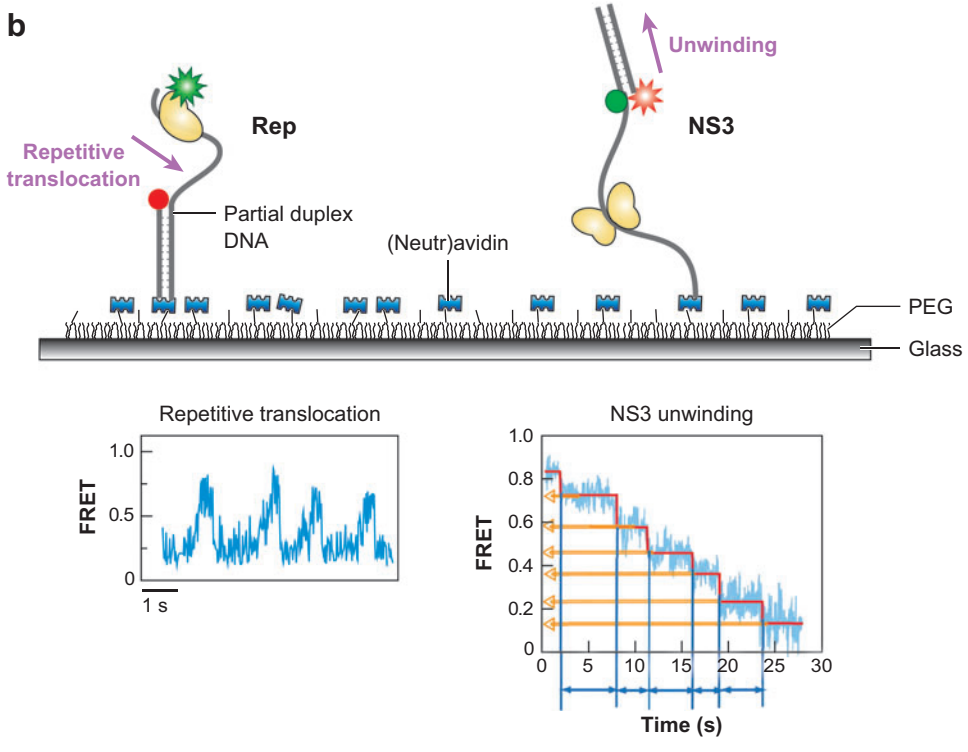

states is best done by using statistical analysis techniques.

Adopting an automated step-finding algorithm originally applied to studying microtubule dynamics (36), the FRET decrease arising from DNA unwinding by an NS3 helicase was analyzed, revealing six discrete steps for 18-base pair DNA (**Figure 2*b***, right) (26). When more complicated bidirectional transitions are the subject of study, elaborate statistical algorithms, such as a hidden Markov modeling (HMM) (37) or likelihood ratio testing (38), are necessary. For instance, the binding and dissociation of several RecA monomers on DNA have been directly observed with SM FRET and analyzed with single-monomer resolution using HMM (27).

FLUORESCENCE LIFETIME MEASUREMENTS

In TCSPC, the interval between excitation and emission of each photon is measured, and a histogram of these intervals is constructed. By using the number of photons at each time point on this histogram, the MLE method estimates the true fluorescence lifetime on the basis of a Poisson or multinomial distribution. The sensitivity and accuracy of these two techniques at low signal levels make them suitable for single-molecule measurements.

More colors. Despite the wealth of information obtained via FRET between two fluorophores, this may not always be enough to characterize a system unambiguously. For example, the aforementioned exchange between two conformers of the Holliday junction has been deciphered on the basis of the relative distance between a pair of arms in any given experiment (15), and the coordinated motion of the four arms was only deduced via a series of complementary measurements. Using a three-color FRET configuration—two acceptors (Cy5 and Cy5.5) and one donor (Cy3)—it was possible to demonstrate the synchronized motion of the DNA arms when the Cy5-labeled arm approached the donor arm at the exact moment that the Cy5.5-labeled arm moved away from the donor arm (39). Similar SM FRET studies were made on a double-stranded (ds) DNA scaffold as well (40–43). The next step of complexity in these studies would be having several (semi-) independent FRET pairs, providing additional information on multisubunit systems.

Fluorescence lifetime measurements. FRET analysis, which is based on the fluorescence lifetime, is an alternative to the intensity-based methods. The advantages include less susceptibility to variation in the excitation intensity, photon-detection efficiency, or spectral cross talk.

Lifetime-based SM FRET on immobilized DNA molecules (44) was recently demonstrated by using time-correlated single-photon counting (TCSPC) along with the maximum likelihood estimator (MLE) analysis method (45, 46). The study showed that the fluorescence lifetime of the donor tetramethylrhodamine switches between two states (2.3 nanosecond versus 1.0 nanosecond) depending on FRET level with the acceptor Cy5. (See the sidebar Fluorescence Lifetime Measurements.)

The lifetime measurement on surface-tethered molecules enjoys the benefit of

Hidden Markov modeling (HMM): a statistical fitting algorithm based on the optimization of Markovian transition processes

Likelihood ratio testing: a model-free method to detect sudden jumps in intensity on the basis of hypothesis tests and likelihood estimation of interphoton arrival times

Fluorescence lifetime: an average period of time a fluorophore spends in an excited state before undergoing relaxation

Figure 2

SM FRET study with surface-tethered molecules. (*a*) Evanescent wave created via total internal reflection fluorescence (TIRF) microscopy. SMs (here Holliday junctions) are tethered via biotin-neutravidin conjugation on the bovine serum albumin (BSA)-coated surface. The conformational dynamics of Holliday junction is shown in a fluorescence time trace (below) (15). (*b*) Studies on proteins necessitate the polyethylene glycol (PEG)-coated surface for better passivation. At left, repetitive translocation of a Rep helicase on single-stranded (ss) DNA is observed via SM FRET (25). At right, stepwise unwinding by an NS3 helicase is visualized via the discrete change in FRET (26).

Annu. Rev. Biochem. 2008.77:51-76. Downloaded from www.annualreviews.org
by Kanazawa University Medical Library Branch on 09/07/10. For personal use only.

Annu. Rev. Biochem. 2008.77:51-76. Downloaded from www.annualreviews.org
by Kanazawa University Medical Library Branch on 09/07/10. For personal use only.

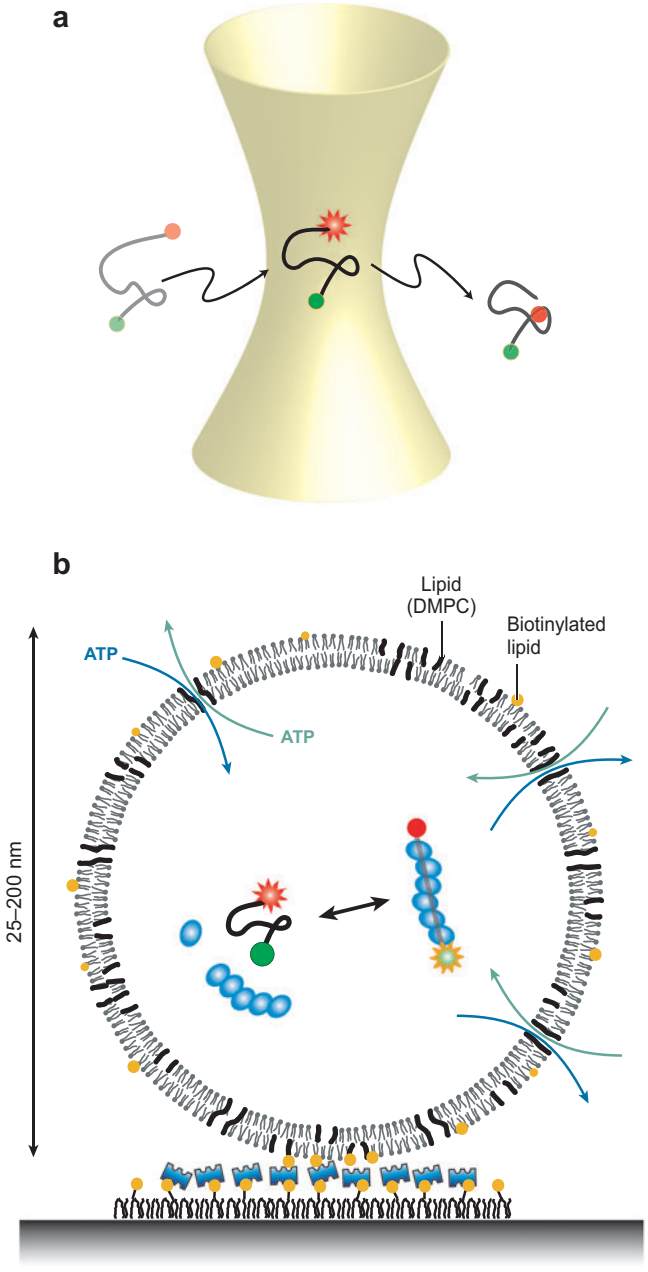

Figure 3

SM FRET study on freely floating molecules. (*a*) In the confocal microscope, a molecule is observed only when it passes through the tightly focused laser beam. (*b*) An immobilized lipid vesicle, containing several RecA proteins and a ssDNA. Small molecules, such as ATP, can freely enter and exit the vesicle via pores (72).

extended observation time. However, because the lifetime measurements require a higher number of photons compared to intensity-based methods, the longevity of the fluorophore has to be sacrificed for better time resolution. It has been shown theoretically (47) and confirmed experimentally (46) that the minimum number of photons needed for fitting a histogram to a single lifetime is between 200 and 1000. With the minimum required number, it is possible to obtain traces with a 10-ms time resolution (44).

TCSPC has also been used for studying other types of molecular quenching mechanisms such as photoinduced electron transfer. Conformational dynamics of individual flavin reductase were investigated via the changes in the fluorescence lifetime of a bound fluorescent substrate, flavin, owing to electron transfer to a nearby aromatic residue (48).

Freely Diffusing Molecules

Although passivation techniques minimize the surface-induced perturbation, the entire problem may be bypassed by detecting fluorescence signal from freely diffusing molecules. This measurement involves collecting bursts of fluorescence photons as each of the SMs diffuses across the tightly focused excitation volume (**Figure 3*a***). After the first demonstration (49), recent developments made this method applicable to many different biological systems, with higher FRET accuracy and with the capability of probing additional physical parameters.

Protein folding. In a recent study of a cold-shock protein labeled at each terminus with Alexa 488 and 594, the intramolecular distance between the dyes was measured at different denaturant (guanidium chloride) concentrations (50). Two characteristic FRET values implied the existence of two thermodynamically stable states (folded and unfolded) with a single shallow free-energy barrier, similar to

chymotrypsin inhibitor 2 (51) and RNAse H (34).

To watch the folding and unfolding process before equilibrium is reached, the fast and efficient mixing of a denaturant and a protein is crucial. Recently, the initial collapse of the cold-shock protein was detected by quickly exchanging a denaturant condition via a microfluidic device (52). Other fast reaction initiation techniques include photochemical triggering (53), temperature jump (54), and nanopipette-based mixing (55).

Insoluble proteins. Membrane proteins can also be studied by reconstituting them with soluble surfactants. In a classic example, doubly labeled F_0F_1-ATP synthase was incorporated in a lipid vesicle membrane (56), which diffused slower because of its size (several hundred milliseconds through the excitation volume), allowing a sufficient time window to record several steps of ATP synthesis. With this capability, the 120° stepwise rotation during both ATP hydrolysis and synthesis was confirmed.

Multiple excitations. By directly exciting the acceptor, it is possible to collect more accurate stoichiometric information. In a scheme called alternating laser excitation (ALEX) (57), donor and acceptor excitations are alternated in the microsecond timescale to allow sufficient time for both dyes to be excited within the excitation volume. Then, the dissociation constant is calculated for a model system, a catabolite activator interacting with DNA, with photons emitted from donor, FRET-excited acceptor, and directly excited acceptor. Additional benefits of ALEX include segregation of a low FRET population from donor-only molecules, which was essential for elucidating the mechanism of transcription initiation (58), and simultaneous collection of parameters necessary for accurate conversion of FRET into distance information (57, 59, 60).

The alternation rate can be as fast as nanoseconds, useful for high time-resolution studies and fluorescence lifetime measurements (61, 62), and as slow as milliseconds (63), applicable to the study of surface-tethered molecules. Recently, three-color alternating excitation was introduced (64) to demonstrate the possibility of elucidating more complex structural information. In principle, additional excitation and emission channels can be added, but the challenge lies in the complexity of data interpretation.

Multiparameter measurements. A fluorescence photon contains valuable information about many parameters including photon energy (fluorescence spectrum), polarization direction (fluorescence anisotropy), photon emission time (fluorescence lifetime), and interphoton emission time (fluorescence correlation). As seen throughout this review, different detection schemes can be combined to harvest useful information from a photon.

Recently this idea was taken to new dimensions, showing that at least eight dimensions of information can be obtained from individual molecules in solution (65). The setup separates fluorescence photons by spectral differences and further by polarization differences. The excitation is performed by a series of short laser pulses. The detected fluorescence signal is routed to a TCSPC unit to measure the fluorescence lifetime or interphoton time. FRET efficiency and molecular stoichiometry may be obtained by a scheme similar to ALEX. These efforts resulted in molecular identification of 16 different fluorescent species, a feat probably impossible if measurement was restricted to one parameter alone, such as intensity-based FRET.

Confined Molecules

Measurement with freely diffusing molecules offers a convenient option for obtaining SM FRET data with the least modification on host molecules. However, several limitations prevail; for example, a protein interaction experiment at high concentration of labeled substrates is hampered by high

Annu. Rev. Biochem. 2008.77:51-76. Downloaded from www.annualreviews.org
by Kanazawa University Medical Library Branch on 09/07/10. For personal use only.

Annu. Rev. Biochem. 2008.77:51-76. Downloaded from www.annualreviews.org
by Kanazawa University Medical Library Branch on 09/07/10. For personal use only.

background. An alternative approach is to confine the freely diffusing molecules within nanocontainers.

Zero-mode waveguide. A method was developed to excite molecules, which are confined within an attoliter volume (10^{-18}), on the basis of a zero-mode metallic waveguide (ZMW) (66). The surface of a ZMW consists of an array of ~100-nm diameter wells on a thin aluminum film (~100 nm) deposited on a fused glass coverslip. No optical modes can propagate through these subwavelength wells, and therefore, the background signal, which would ordinarily emerge from molecules in bulk solution, is greatly minimized. Single T7 DNA polymerases were adsorbed on the bottom glass surface within the ZMW, and binding of fluorescently modified nucleotides to the polymerase during DNA synthesis was detected at the SM level, although not yet via FRET, even at ~10-μM concentration. The surface of the ZMW can be passivated via coating with lipid bilayers (67). The array of apertures and the open configuration allow an easy exchange of buffer, making the ZMW a strong candidate for high-throughput measurements such as massively parallel SM-DNA sequencing (68).

Vesicle encapsulation. A limitation of the ZMW is the very short residence time of unbound fluorescence species in the imaging volume (much less than a millisecond). A promising alternative is to confine SMs inside sealed containers, for example, encapsulating a fluorescently labeled protein within a 100-nm unilamellar lipid vesicle that is tethered to the supported membrane bilayer surface (69). In this study, encapsulation of single proteins was confirmed by the number of photobleaching events from the immobilized vesicles. This approach should work well for any molecule that does not strongly interact with the membrane. For example, complex conformational fluctuation of adenylate kinase was observed inside a vesicle (70). The same approach was also used to show that the static and dynamic heterogeneities in the folding dynamics of the hairpin ribozyme and G-quadruplex were not from surface artifacts (18, 71).

Porous vesicle. One serious drawback with vesicle encapsulation is that the lipid membrane is impermeable to most of the ions and small molecules, limiting its application to studying SM dynamics in equilibrium. This barrier could be overcome by utilizing the porous nature of a lipid membrane near the gel-fluid transition temperature (T_m) (**Figure 3*b***) (72). The RecA protein and a DNA strand were encapsulated within a vesicle made out of dimiristoylphosphatidylcholine ($T_m = 23°C$), which was permeable to small molecules, such as ATP, at room temperature. Therefore, the dynamic interaction between the RecA and the DNA could be readily modulated by flowing ATP and its analogs through the membrane pores while the proteins and DNA molecules stayed within the surface-tethered porous vesicles.

Applications. Because molecules inside a vesicle are confined within about an attoliter (10^{-18}) volume, a high effective concentration (micromolar range) may be achieved without hampering SM detection (72). Therefore, the vesicle encapsulation method may be useful in studying the molecular crowding effect found in cellular environments (73, 74). In addition, the unique capability of studying the repeated interaction between the same set of molecules may help address some of the elusive issues in SM enzymology, such as molecular heterogeneities and memory effects (5, 16, 75, 76).

TRACKING

FRET reports on the relative distance changes in the center of the mass frame of the molecules being studied. The following two subsections cover SM fluorescence techniques that can measure molecular position (translocation) and molecular orientation (rotation) in the laboratory frame.

Translocation

Studying the movements of processive motor proteins typically requires tracking over distances much longer than the Förster radius, hence necessitating techniques different from FRET. Recent efforts in SPT have been concentrated on this problem, particularly when the linear track of the motor protein is laid on a surface. These efforts have resulted in an impressive nanometer accuracy of localization, via wide-field fluorescence microscopy, for many microns of motor translocation.

Brief history. Earlier room temperature SPT experiments were concentrated on measuring diffusion coefficients of fluorophores in solution or within lipid membranes. By using conventional epifluorescence microscopy, high excitation power (~50 kW/cm^2), and a liquid nitrogen-cooled CCD, it was possible to track a single rhodamine molecule embedded in a phospholipid membrane with 30-nm spatial accuracy at 5 ms-time resolution via fitting a two-dimensional (2D) Gaussian curve to the point spread function of fluorophore emission (**Figure 4*b***) (77). This fitting method served as a model for many subsequent studies.

In an important study, the limitations of SPT were systematically analyzed in terms of photon shot noise, pixelation, and background noise (78). The study concluded that the localization precision scales as $1/\sqrt{N}$ in the shot noise-limited case and as $1/N$ in the background noise-limited case, where N is the number of collected photons. Therefore, it was shown theoretically and experimentally, although on intensely fluorescent beads, that nanometer precision of SM localization was possible with many enough photons and low enough background.

Fluorescence imaging with one-nanometer accuracy. These earlier pioneering approaches were merged to track a myosin V protein, labeled with a single Cy3 or rhodamine dye, while it was moving on an actin filament (**Figure 4*a***) (79). An oxygen scavenger system (80) and a triplet-state quencher (81) were used together with TIRF microscopy to reduce the background and to enhance the photostability and brightness. With these improvements, as many as 20,000 photons/second were collected from a single dye, making 1.5-nm spatial accuracy with 0.5 s time resolution possible (for >60 s observation) (**Figure 4*c***). This study provided the most definitive proof that myosin V moves hand over hand.

This work (79) has inspired many other studies. Two groups extended this method to colocalizing two fluorophores with different colors and were able to track both heads of the myosin V dimer simultaneously (82, 83). In one study (82), two heads of the myosin V dimer were labeled with quantum dots (Q-dots) that could be excited with the same laser but had different emission peaks (565 nm and 655 nm), a scheme demonstrated earlier in a nonbiological setting (84), and the heads were colocalized with 6-nm accuracy (**Figure 4*d***). In a similar study, Cy3 and Cy5 were used to label the heads, and better than 10-nm colocalization was obtained (83).

Measuring the distances between multiple fluorophores without the need for distinguishable colors, which were within 10 nm or more apart from each other, was also achieved by utilizing sequential photobleaching of the dyes (85, 86). This method was applied to measure the interhead distance of myosin VI dimer (87), a measurement that would traditionally be in the realm of more elaborate techniques such as electron microscopy.

Oxygen scavenger system: generally composed of glucose oxidase and catalase, which converts oxygen and glucose molecules into gluconic acids

Q-dot: quantum dot

Rotational Motion

In many biological systems, the orientation of certain domains or their rotational motion underlies their enzymatic activity. In these systems, such as the F1-ATPase (**Figure 5*b***), their function can be determined by the rotational movements of subdomains using polarization microscopy (88).

Annu. Rev. Biochem. 2008.77:51-76. Downloaded from www.annualreviews.org
by Kanazawa University Medical Library Branch on 09/07/10. For personal use only.

Annu. Rev. Biochem. 2008.77:51-76. Downloaded from www.annualreviews.org
by Kanazawa University Medical Library Branch on 09/07/10. For personal use only.

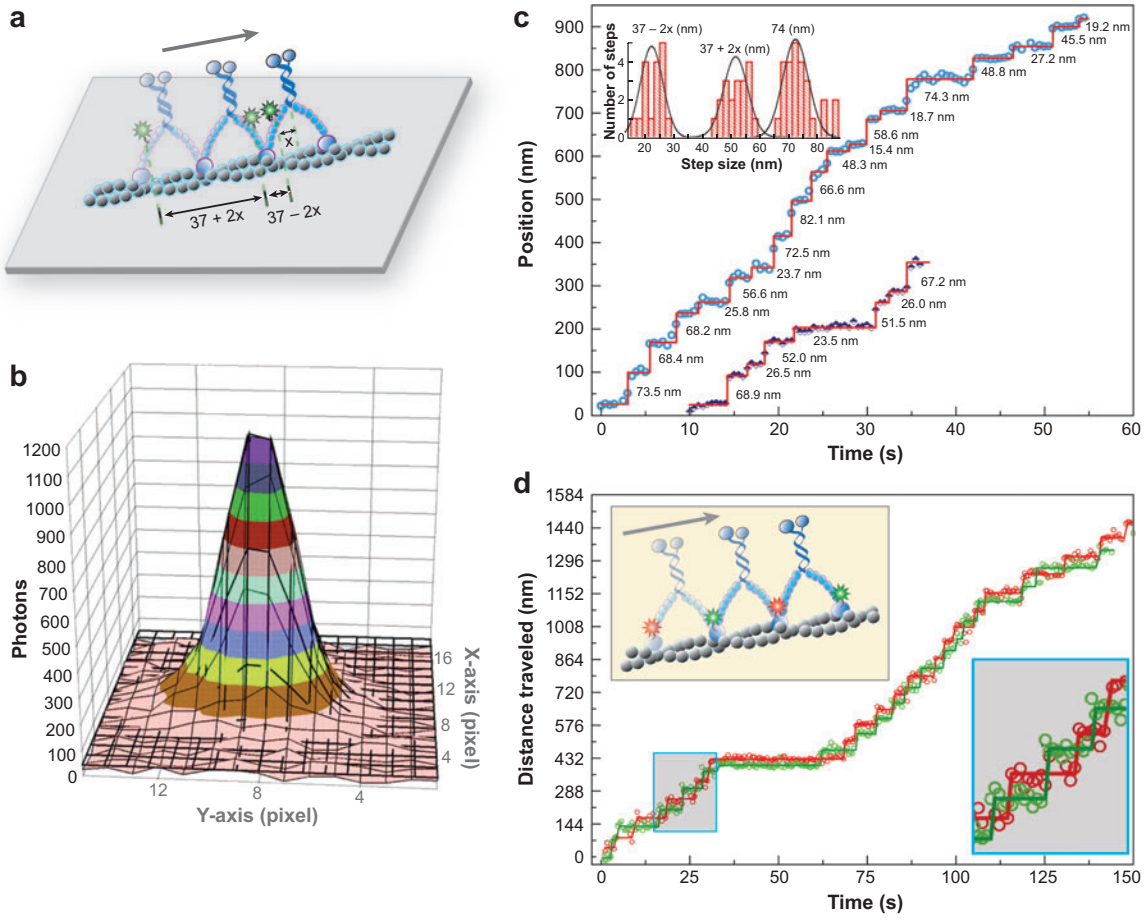

Figure 4

Single-particle tracking of a motor protein. (*a*) The hand-over-hand mechanism predicts a sequence of large ($37 + 2x$ nm) and small ($37 - 2x$ nm) steps. (*b*) Fluorescence localization is achieved with nanometer accuracy by the point spread function fitted with a 2D Gaussian curve (79). (*c*) Shown is the stepwise motility (52 and 23 nm) of the myosin V labeled with bifunctional rhodamine (79). Although this was originally analyzed by a visual inspection, later studies analyzed similar data using statistical methods, such as the t-test and HMM (149). (*d*) A myosin V, labeled with quantum dot (Q-dot) 565 on one head and Q-dot 655 on the other head, shows the sequential stepping of heads (82).

Principle. The probability that an excitation photon would be absorbed by a fluorophore is proportional to $\cos^2(\varphi)$, where φ is the angle between the polarization axis of the excitation light and that of the fluorophore dipole (**Figure 5*a***, left). Similarly, in the case of polarization-dependent detection, i.e., if a polarizer is placed before the detector, the probability of detecting an emitted photon is proportional to $\cos^2(\theta)$, where θ is the angle between the emission dipole of the fluorophore and the transmission axis of the polarizer (**Figure 5*a***, right). Hence, the intensity of the detected signal, practically limited by a millisecond or longer integration time, depends on the orientation of the fluorophore. If this method is combined with a lifetime measurement, it is possible to infer rotational motions at nanosecond timescale.

Annu. Rev. Biochem. 2008.77:51-76. Downloaded from www.annualreviews.org
by Kanazawa University Medical Library Branch on 09/07/10. For personal use only.

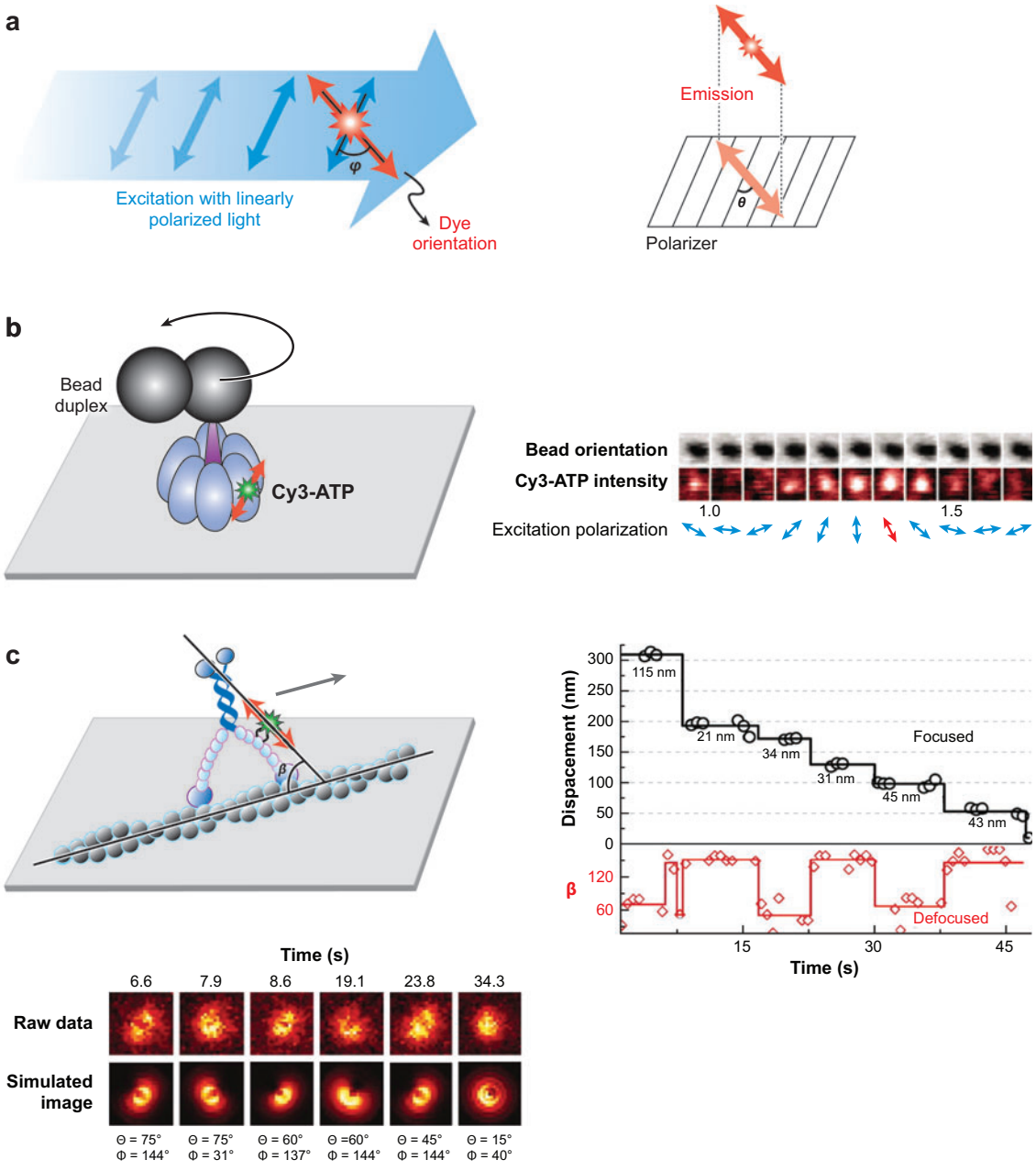

Figure 5

Polarization microscopy. (*a*) A dye is illustrated at an angle φ with the laser polarization and θ with the polarizer in front of a detector, the relevant geometries for polarization microscopy. (*b*) Cy3 orientation is determined from its polarization, and the F1-ATPase activity is independently monitored through the rotation of an attached bead duplex (91). (*c*) The angle β between the dye on the myosin light chain domain and the actin filament is measured by defocused imaging. (*right*) Both the position and angle are detected by alternating between focused imaging for translocation and defocused imaging for rotation. (*bottom*) An example of a polarization imaging data with the corresponding simulation shown (94).

LCD: light chain domain

Polarization intensity trajectory. In the first biological application of a SM polarization study, Sase et al. (89) studied the axial rotation of myosin around the actin helix. Linearly polarized light excited the actin filaments, which were sparsely labeled with rhodamine molecules that were immobile relative to the actin. The orientation of these filaments while sliding on surface-bound myosins was observed via the change in rhodamine orientation. Actin has a helical pitch of 72 nm, and the study surprisingly found that the actin filament completed a full rotation in approximately 1 μm, suggesting that myosin does not follow the actin helical pitch but it rather skips many protomers while walking.

Advanced polarization intensity trajectory techniques. Several issues that can complicate a SM orientation determination should be noted. (*a*) Unless the fluorophore is rigidly attached to the host molecule, it will wobble within a certain cone of angles, compromising the accuracy of angle measurement. (*b*) It is not possible to extract orientation information about the axis perpendicular to the polarization plane of the excitation beam. (*c*) Even within that plane, the angles φ and 180-φ are degenerate, i.e., $\cos^2(\varphi) = \cos^2(180\text{-}\varphi)$, and hence, both orientations result in the same signal.

These issues were addressed by attaching a bis-sulfonerhodamine (BSR) to a kinesin protein at two points, which significantly reduces the wobbling problem (90). In addition, excitation light polarized along two sets of orthogonal axes (0°–90° and 45°–135°) was used to reduce the inherent degeneracies of single polarization. With these improvements, it was shown that kinesin adopts a highly mobile state while in the ADP-bound form, unlike other nucleotide states.

In the case of myosin V, SM polarization showed that the light chain domain (LCD) tilts between two discrete angles during the protein translocation (12). LCD was labeled with BSR; four different polarization axes, sequentially modulated by a Pockels cell, were used for the excitation light, and two different polarization axes were detected. The angle between the trailing and leading LCD was measured and shown to be consistent with the hand-over-hand walking mechanism.

In addition to pure polarization measurements, polarization information can be correlated with other observables simultaneously measured from the SM. A great example is the rotary motor F1-ATPase (**Figure 5*b***) (91). The rotation of γ subunit was detected via bright-field imaging of a bead duplex bound to the motor, whereas polarization microscopy was used for detecting the binding and dissociation of Cy3-conjugated ATP and for identifying the binding site.

Polarization imaging. All the studies, reviewed so far, used the polarization intensity trajectory technique. Another approach, polarization imaging, reports three-dimensional (3D) orientation of the fluorophore via the unique fluorescence intensity patterns that depend on the direction of excitation polarization (92). This technique lacks the high temporal resolution that the trajectory technique possesses but it requires a simpler experimental setup and is capable of providing more accurate information on the molecular orientation.

In an early application of polarization imaging, it was shown that a single DiI fluorophore with the polarization axis aligned along the z-axis (optic axis) displays a spread out doughnut-shaped emission pattern when excited with light polarized within the (x-y) plane (93).

The first biological application of this observation, an emission pattern that depends on the 3D orientation of a dye, was done on a myosin construct (**Figure 5*c***) (94), similar to that of Forkey et al. (12). In this study, Toprak et al. toggled the imaging plane between focused, for SPT, and defocused, to extract the orientation information. The time trace clearly showed that the orientation change of the LCD was associated with translocation of the motor (**Figure 5*c***, right) (94). The

Annu. Rev. Biochem. 2008.77:51-76. Downloaded from www.annualreviews.org
by Kanazawa University Medical Library Branch on 09/07/10. For personal use only.

70° measured between trailing and leading heads eliminated the degeneracies of previous measurements.

TRACKING IN LIVE CELLS

In vitro SM techniques are now established as powerful biochemical tools that can reveal the dynamic nature of proteins and nucleic acids. By contrast, SM imaging in live cells still remains challenging owing to several inherent difficulties, even though they keep attracting many SM researchers because of their biological importance (95). One of the holdbacks for in vivo SM studies is the low SNR, which is primarily caused by cellular autofluorescence, such as those of flavonoids (yellow and green emissions, 10^6–10^8 molecules/cell) (96). The rapid diffusion or translocation of molecules in three dimensions is another challenge, which necessitates high time resolution (See sidebar of Imaging in Live Cells).

Membrane Proteins

The SNR can be improved by corralling SMs in a 2D plane, such as a plasma membrane, that prevents their diffusion out of the focal plane (**Figure 6*a***) and/or by exciting a cell with an evanescent wave, which minimizes the cellular autofluorescence (97).

Lateral diffusion and stoichiometry. Iino et al. (98) tagged a transmembrane protein, E-cadherin, with GFP and distinguished the individual protein clusters in diffusion (**Figure 6*a***, bottom left). By tracking the clusters with 33-ms time resolution, their diffusion constants were measured, and by using their quantized fluorescence intensity, the cluster stochiometry was determined. Similar characterization was done for other transmembrane proteins (99) and for anchored proteins, such as Ras (100, 101), tagged with eYFP or GFP. This approach was applied also to signaling proteins in a T cell, and the protein-protein interactions were inferred as the origin of the plasma membrane microdomains (102). In addition, this protein identification method provides a straightforward way of counting the subunits of a protein complex (98–100). For example, the subunits of channel and receptor proteins tagged with GFP were counted directly by the number of discrete photobleaching steps (103).

A higher SNR was achieved by using synthetic dyes as demonstrated by the work on the epidermal growth factor (EGF) receptor (104). Because the receptor binds extracellular EGF, the movement and dimerization of the receptors were observed through the dye-labeled EGF arriving from outside the cell (**Figure 6*a***, bottom right). This method was applied to similar systems of cAMP receptors (105) and to peptide-binding proteins (106). Further signal improvement was achieved in studying glycine receptors by tagging them with Q-dots, which made tracking over extended periods possible (>20 min) (107).

Protein translation. Because translation occurs in the 3D volume of cytoplasm, a protein's birth is much more difficult to detect than the activity of a membrane protein. Yu et al. (108) recently overcame this difficulty by exploiting the membrane protein, Tsr. A model protein, Venus, becomes fluorescent after translation and maturation (~7 min). Once Tsr-tagged Venus becomes anchored onto a plasma membrane, the localized fluorescence signal is unambiguously detected. This near real-time

IMAGING IN LIVE CELLS

To visualize SMs in live cells, several conditions should be satisfied. First, the high autofluorescence of the cell requires bright fluorophores and/or evanescent wave excitation. Second, the crowded nature of the cell necessitates high specificity in labeling the molecule of interest. Third, the copy number of the molecules should remain low enough to avoid colocalization of multiple copies within the diffraction limit. Finally, the high ATP and oxygen concentrations of the cellular environment compel high temporal resolution and low doses of excitation, respectively.

Annu. Rev. Biochem. 2008.77:51-76. Downloaded from www.annualreviews.org
by Kanazawa University Medical Library Branch on 09/07/10. For personal use only.

Annu. Rev. Biochem. 2008.77:51-76. Downloaded from www.annualreviews.org
by Kanazawa University Medical Library Branch on 09/07/10. For personal use only.

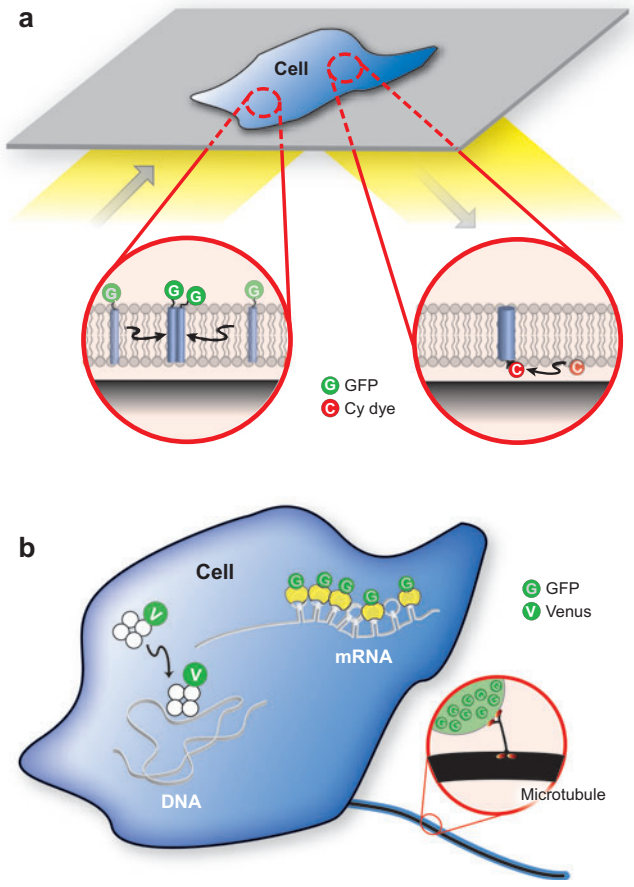

Figure 6

Live cell imaging (*a*) for tracking membrane proteins in lateral diffusion via total internal reflection microscopy, (*b*) for detecting a transcription factor binding onto DNA (*left*) (109); for identifying the presence of an mRNA in the cytoplasm (*top*) (115); and for tracking a motor protein (*right*) (111). Abbreviation: GFP, green fluorescent protein.

identification of the translation event (3-min time resolution) revealed the bursting nature of translation—several proteins per mRNA.

Cytoplasmic Proteins

A large portion of cellular activities occurs in the cytoplasm rather than on the plasma membrane. The technical difficulties in identifying and tracking the cytoplasmic proteins in random 3D diffusion have been partially answered by several studies.

Transcription factor binding. Carrying out the idea of detection by immobilization, Elf et al. (109) watched the activity of a single Venus-tagged LacI transcription factor. Although not completely stationary, a chromosomal DNA provided an effective immobile binding site (*lac* operator) to the LacI repressor, thereby making SM detection possible (**Figure 6*b***, left). The snapshots taken (1–1000-ms time resolution) helped measure the timescales of the binding and the dissociation of the LacI to and from a target sequence and that of the search process on a nonspecific DNA (several milliseconds at a time).

Transport through the nuclear pore complex. Another type of localization naturally occurs when a substrate is transported through the nuclear pore complex (NPC) (110). Yang et al. tagged a nuclear localization sequence with synthetic dyes. The interaction of this substrate with the NPC temporarily localized its movement within 200 nm, enabling the identification of the fluorescence signal with high spatial (30 nm) and temporal (3 ms) resolution. The study concluded that transport through the NPC occurs as a random walk.

Motor proteins on linear tracks. Two groups demonstrated the SPT capability for kinesin and dynein motor proteins by tracking peroxisomes tagged with ~1000 eGFPs (**Figure 6*b***, right) and endocytosed vesicles containing Q-dot aggregates, respectively (111, 112). Both studies reported 8-nm steps typical of single kinesin or dynein activity, in addition to 16 or 24 nm jumps, reminiscent of multimotor activity, toward both ends of the microtubule with a millisecond or better time resolution. However, only a very tiny fraction of time traces in both studies showed clearly identifiable steps, so it is still unclear whether these large organelles move in 8-nm steps when supported by a large number of motors, which would be the case in the cell. In fact, a recent in vitro study suggested that

multiple motors bound to the cargo result in fractional steps (113).

Other Single Objects

Single-particle detection in live cells is not limited only to proteins. By attaching many copies of fluorophores to the same objects, tracking was also realized for mRNA molecules and viruses.

RNA transcript. Unlike proteins, RNA can not be covalently labeled with endogenous fluorophores. Singer and coworkers (114) pioneered the real-time visualization for single RNA molecules with an MS2-coat protein. The MS2 protein has high specificity and affinity toward a small RNA hairpin. When a GFP-fused MS2 protein is constitutively expressed in a cell, the presence of an RNA transcript tagged with hairpin repeats is immediately identified by the strong, localized signal from the multiple GFP-fused MS2 proteins bound to it (**Figure 6*b***, top). This made it possible to observe the movement of single RNA transcripts in a mammalian cell in real time (10 ms time resolution) (115).

The same technique, but with careful modifications, was successfully applied to a smaller organism, *Escherichia coli*, by Golding & Cox (116). In this study, not only the diffusion motion of an RNA transcript was tracked (116) but also the creation of a transcript in near real time was observed, discovering the stochastic nature of transcription (30 s time resolution) (117). A similar transcription burst was observed in eukaryotes (118).

Virus. Finally, a virus inside a live cell was tracked as a single object. Seisenberger et al. (119) first observed a Cy5-tagged AAV virus interacting with a HeLa cell. They showed how efficiently the virus fuses into the cell, and how fast it diffuses and is transported inside the cell. More recently, Zhuang and coworkers (120, 121) have investigated the endocytosis mechanism of influenza virus, whose membrane was labeled with multiple dyes. The real-time tracking (0.5 s time resolution) of the virus has identified several distinct endocytic pathways and has quantitatively characterized the detailed process of endosome transport.

MEASUREMENTS UNDER FORCE

Force is recognized now as an important determinant of biochemical reactions. Recently, mechanical manipulation and detection were combined with SM fluorescence techniques, opening up new avenues of investigation. A pioneering work in this direction was the simultaneous detection of myosin power stroke via force spectroscopy and of ATP binding and dissociation via fluorescence imaging (122).

Optical Tweezers

A force between 0.1–100 piconewton (pN) can be applied with high accuracy to a SM through a DNA linker that is tethered to an optically trapped bead (**Figure 7*a***). When incorporated into fluorescence microscopy, force is exerted on the SM whose fluorescence signal is being observed. A demonstration of this principle was made by observing the force-induced dsDNA unzipping via a reduction in the fluorescence quenching of two closely spaced rhodamines (123). The first design suffered from accelerated photobleaching caused by an intense infrared trapping beam; this was later overcome by microsecond-timescale alternation between the trapping and the excitation beams. This improvement greatly reduced the severe photobleaching without hampering the temporal resolution (124). Several cycles of force-induced DNA hairpin folding and unfolding, through FRET, were observed using this technique (125).

Another way of avoiding the fast photobleaching problem is to spatially separate the excitation and the trapping laser beams (126). Hohng et al. have shown that when two beams are separated by a 16-μm linker

Annu. Rev. Biochem. 2008.77:51-76. Downloaded from www.annualreviews.org
by Kanazawa University Medical Library Branch on 09/07/10. For personal use only.

Annu. Rev. Biochem. 2008.77:51-76. Downloaded from www.annualreviews.org
by Kanazawa University Medical Library Branch on 09/07/10. For personal use only.

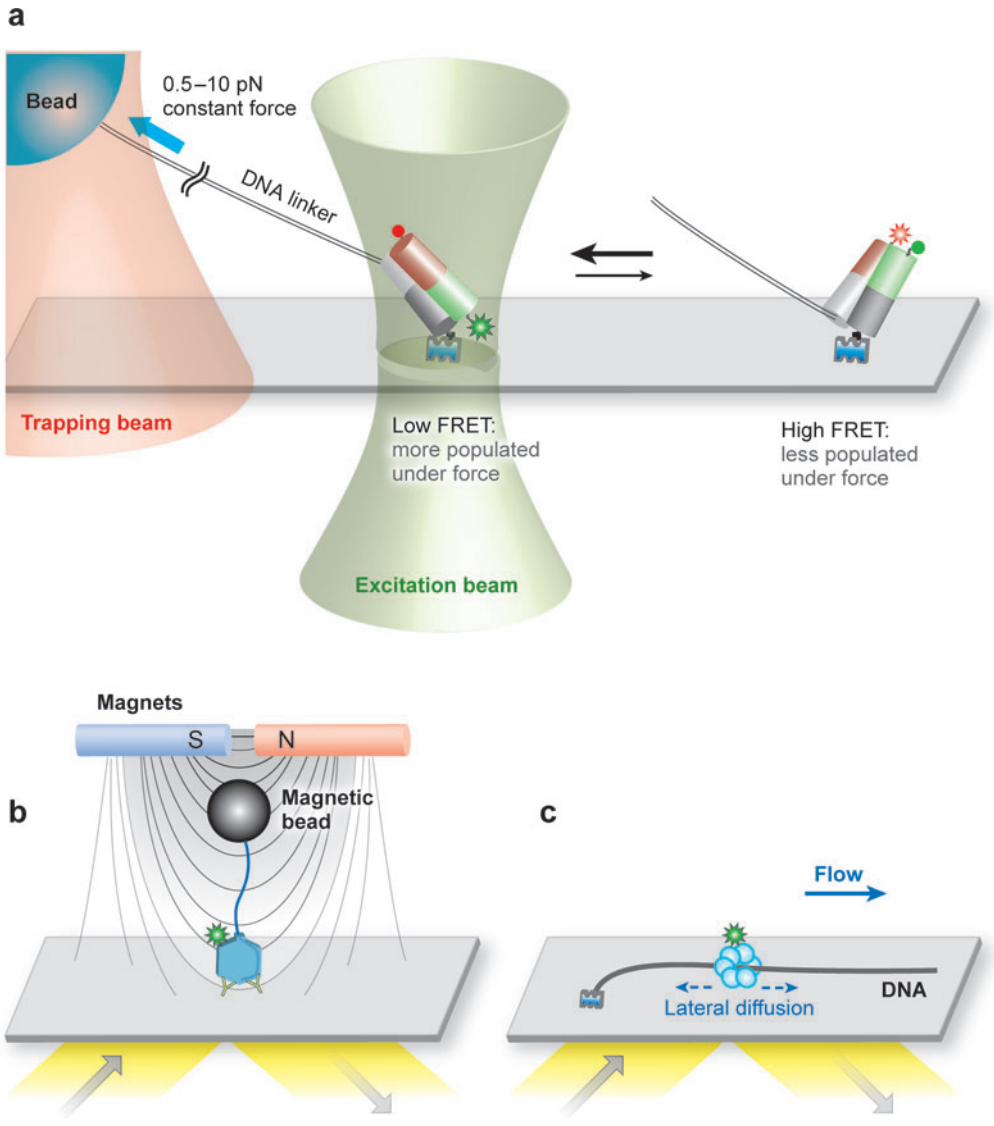

Figure 7

Fluorescence microscopy combined with (*a*) optical tweezers (126), (*b*) magnetic tweezers (129), and (*c*) laminar flow methods (131).

(λ-DNA), the dynamics of the Holliday junction can be observed even with the trapping beam on (**Figure 7*a***). As described above (**Figure 2*a***), the junction undergoes conformational dynamics between the two stacked forms along its energy landscape. When the junction is pulled in a certain way, one conformation becomes energetically more favorable than the other. Exploration over the physical energy landscape by pulling in three different directions with a range of forces (0.3–5 pN) led to the structural determination of the elusive transition states. Another combined technique, although force and fluorescence were not used simultaneously, was employed for FRET-based identification of a

fully assembled ribosome complex to be studied via force measurements (127).

Magnetic Tweezers

A similar magnitude of force can be applied with magnetic tweezers, which are simpler to implement and do not require strong light sources that interfere with fluorescence detection. TIRF microscopy was combined with magnetic tweezers to build a calibration curve of FRET values between the dyes at the ends of a ssDNA versus pN forces that stretch DNA (128).

In another configuration, magnetic tweezers were used as a positive control for SM fluorescence polarization analysis (**Figure 7*b***) (129). A putative rotary motor (DNA-packing a gp8 dodecamer, located at the neck of a φ29 virus) was labeled with a dye. Because the dye was linearly polarized and the capsid of the virus was affixed onto the surface via multiple points, the polarization change of the fluorescence signal was expected to report on the possible rotational motion of the dodecamer. While the activity of the viral DNA packing was being watched by the decrease in the length of DNA tethered to a magnetic bead, the orientation of the motor was checked by TIRF polarization microscopy. No rotational motion of the dodecamer was observed, ruling out the connector-rotation model proposed earlier.

Magnetic tweezers currently do not have as high temporal and spatial resolution as optical tweezers but are capable of applying the torque that is necessary for introducing supercoils on DNA (130). A yet-to-be-achieved but sure-to-be-important goal is to measure how conformations of DNA-bound proteins are affected by the supercoiling state of DNA, using a torque-fluorescence combination.

Laminar Flow

Translocation of dye-labeled single proteins on DNA can be traced over a long distance by SM fluorescence techniques. Precise tracking requires the naturally coiled DNA to be stretched out. Optical and magnetic tweezers are useful for DNA stretching, but they are time consuming and difficult to implement. Laminar flow is a practical alternative because many DNA molecules can be stretched simultaneously without great effort (33).

With surface-tethered λ-DNA molecules stretched by laminar flow, Granéli et al. (131) showed that a complex of Alexa 555-labeled Rad51, a recombinase, diffuses along the ds-DNA (**Figure 7*c***). They were able to observe dozens of stretched DNA molecules in parallel, called "a DNA curtain," and could show with a statistically sufficient number of events that the binding of Rad51 is independent of the DNA sequence. A similar observation was made by a labeled hOgg, a base-excision DNA-repair protein (132). The flow-based assay is also optimal for watching ATP-driven translocation, such as the processive motion of Snf2 family chromatin-remodeling proteins—a fluorescein-labeled Rad54 (133) and a Q-dot-labeled Rdh54 (134).

Finally, this technique has been also useful in visualizing the protein polymerization on DNA by eGFP-labeled MuB, a Mu transposition-related protein (135), and by carboxyfluorescein-labeled RecA (136).

Magnetic tweezers: a method of trapping and manipulating a magnetic bead with a strong magnetic field

Optical tweezers: an optical method of trapping and manipulating a transparent object with a tightly focused laser beam

Laminar flow: a fluid stream at low Reynolds number and free from turbulence

FINAL CONSIDERATIONS

We close our survey with considerations on the fluorescence properties relevant to SM experiments.

SM photon emission rate is ultimately limited by excitation saturation, which occurs when the excitation rate approaches the relaxation rate of a fluorophore, typically one per a few nanoseconds. That is, when saturation is reached, 100 photons, which is a reasonable number for determining FRET efficiency, may be detected in less than 10 μs assuming 10% detection efficiency. In reality, molecular shelving in the triplet state, with a lifetime of microseconds or longer, limits the time resolution to about 100 μs or longer,

Annu. Rev. Biochem. 2008.77:51-76. Downloaded from www.annualreviews.org
by Kanazawa University Medical Library Branch on 09/07/10. For personal use only.

depending on the availability of triplet-state quenchers.

Photobleaching puts another practical limit on how high excitation can be. Photobleaching irreversibly inactivates the fluorophore either by (*a*) the oxidation reaction between the excited fluorophore in the triplet state and the reactive species nearby (137, 138) or (*b*) the excitation of the molecule already in the excited state, possibly leading to an unstable form (139, 140). Both mechanisms would reduce the total number of photons emitted before photobleaching, called N_{pb}, as excitation becomes intense. This can be an additional limiting factor determining the practical time resolution. Several efforts to maximize N_{pb} have been made (10^5–10^6 at best). These include (*a*) reducing the excitation rate to avoid the nonlinear effect discussed above, (*b*) using pulse excitation to avoid the double excitation of an excited fluorophore (141), (*c*) removing reactive oxygen species by the oxygen scavenger system (80), and (*d*) using triplet-state quenchers, such as the popular β-mercaptoethanol (BME) or the water-soluble vitamin E analog, Trolox (81).

Photoblinking is a reversible darkening of a fluorophore. The main mechanisms behind photoblinking are the severe reductions in fluorescence quantum yield, which are due to (*a*) the phototransition between the singlet and the triplet states (called the excited state transition) (142) or (*b*) the switching between the photoactive and the photoinactive forms of the molecule as seen in the case of Cy5 (called the ground state transition) (143). These not only reduce the efficiency of data acquisition owing to a low duty cycle but also may lead to artifacts that are difficult to discern with untrained eyes. Triplet-state quenchers reduce the problem of a prolonged triplet-state lifetime upon oxygen removal but can cause side effects such as the slow blinking of Cy5 (81, 144) induced by BME. Trolox is a much better alternative to BME and allows nonblinking and long-lasting imaging of popular cyanine dyes without any side effect (81).

In the past decade, semiconductor nanocrystals known as Q-dots emerged as another promising class of fluorophores (145). They are superior to organic dyes in several aspects, including, most importantly for SM measurements, high photodestruction resistance and brightness. Advances in surface chemistry made it possible to easily conjugate Q-dots to proteins and oligonucleotides of interest (for more details see References 145 and 146). In addition to their growing popularity in live cell and tissue imaging, Q-dots found their place in SPT, as reviewed in the previous section. Furthermore, a Q-dot was used as a FRET donor to observe conformational changes of a Holliday junction (147), spurred by the discovery that Q-dot blinking can be chemically suppressed (148). However, the large size of commercial Q-dots and the lack of monovalent chemistry need to be overcome before one witnesses a much broader use of Q-dots in SM measurements.

CONCLUSION

SM methodologies are still evolving and branching out. A few items on the agenda of SM biophysicists for the following years are: making in vivo and in situ measurements more accessible, combining multiple techniques, pushing down spatial and temporal resolution, and designing better probes that provide longer and faster measurements under physiological conditions. In particular, essential for expanding SPT capabilities for 3D or live cell measurements are brighter and more stable fluorophores; smaller Q-dots; and faster, more efficient probes.

Beyond these technical feats, SM biophysics has an even grander challenge to overcome: whether it will be able to take its place in the arsenal of general biology tools or remain as a powerful yet specialized tool. There is no doubt that a distribution explains a system better than just its mean; however, whether the effort spent in getting this extra information is affordable by a general biologist is the

Annu. Rev. Biochem. 2008.77:51-76. Downloaded from www.annualreviews.org
by Kanazawa University Medical Library Branch on 09/07/10. For personal use only.

real factor that will determine the future of the field. Considering the exponential growth of the field in the recent years, we are optimistic that a favorable outcome will be realized.

SUMMARY POINTS

1. SM FRET has been utilized in studying the molecular dynamics of many important biological systems.
2. Nanometer accuracy has been achieved in tracking a single fluorophore.
3. The 3D orientation of a SM can be determined via SM fluorescence polarization.
4. SM tracking in live cells is possible but not yet at the desired level.
5. Combining fluorescence techniques with force spectroscopy has been demonstrated.
6. There have been key technical advances in detection technology and in making fluorophores brighter and more photostable.

DISCLOSURE STATEMENT

The authors are not aware of any biases that might be perceived as affecting the objectivity of this review.

ACKNOWLEDGMENTS

This work was supported by the National Institutes of Health (R01-GM074526 and R01-GM065367) and by the National Sciences Foundation CAREER Award (PHY01–34916).

LITERATURE CITED

1. Moerner WE, Kador L. 1989. *Phys. Rev. Lett.* 62:2535–38
2. **Orrit M, Bernard J. 1990. *Phys. Rev. Lett.* 65:2716–19**
3. Betzig E, Chichester RJ. 1993. *Science* 262:1422–25
4. **Funatsu T, Harada Y, Tokunaga M, Saito K, Yanagida T. 1995. *Nature* 374:555–59**
5. Lu HP, Xun L, Xie XS. 1998. *Science* 282:1877–82
6. Shaner NC, Steinbach PA, Tsien RY. 2005. *Nat. Methods* 2:905–9
7. Giepmans BNG, Adams SR, Ellisman MH, Tsien RY. 2006. *Science* 312:217–24
8. Mujumdar RB, Ernst LA, Mujumdar SR, Lewis CJ, Waggoner AS. 1993. *Bioconjug. Chem.* 4:105–11
9. Zhuang X, Bartley LE, Babcock HP, Russell R, Ha T, et al. 2000. *Science* 288:2048–51
10. Ha T. 2001. *Methods* 25:78–86
11. **Ha T, Enderle T, Ogletree DF, Chemla DS, Selvin PR, Weiss S. 1996. *Proc. Natl. Acad. Sci. USA* 93:6264–68**
12. Forkey JN, Quinlan ME, Shaw MA, Corrie JE, Goldman YE. 2003. *Nature* 422:399–404
13. Drexhage KH. 1990. In *Topics in Applied Physics*, ed. FP Schäfer, pp. 155–200. Berlin: Springer-Verlag
14. Stryer L. 1978. *Annu. Rev. Biochem.* 47:819–46
15. McKinney SA, Declais AC, Lilley DM, Ha T. 2003. *Nat. Struct. Biol.* 10:93–97
16. Tan E, Wilson TJ, Nahas MK, Clegg RM, Lilley DM, Ha T. 2003. *Proc. Natl. Acad. Sci. USA* 100:9308–13

First experiment detecting single molecules via fluorescence.

First experiment detecting single-molecule fluorescence in aqua and at room temperature.

First experiment detecting FRET at the single-molecule level.

Annu. Rev. Biochem. 2008.77:51-76. Downloaded from www.annualreviews.org
by Kanazawa University Medical Library Branch on 09/07/10. For personal use only.

Annu. Rev. Biochem. 2008.77:51-76. Downloaded from www.annualreviews.org
by Kanazawa University Medical Library Branch on 09/07/10. For personal use only.

17. Liu S, Bokinsky G, Walter NG, Zhuang X. 2007. *Proc. Natl. Acad. Sci. USA* 104:12634–39
18. Lee JY, Okumus B, Kim DS, Ha T. 2005. *Proc. Natl. Acad. Sci. USA* 102:18938–43
19. McKinney SA, Freeman AD, Lilley DM, Ha T. 2005. *Proc. Natl. Acad. Sci. USA* 102:5715–20
20. Nahas MK, Wilson TJ, Hohng S, Jarvie K, Lilley DM, Ha T. 2004. *Nat. Struct. Mol. Biol.* 11:1107–13
21. Lee TH, Lapidus LJ, Zhao W, Travers KJ, Herschlag D, Chu S. 2007. *Biophys. J.* 92:3275–83
22. Kim HD, Nienhaus GU, Ha T, Orr JW, Williamson JR, Chu S. 2002. *Proc. Natl. Acad. Sci. USA* 99:4284–89
23. Ha T, Rasnik I, Cheng W, Babcock HP, Gauss GH, et al. 2002. *Nature* 419:638–41
24. Rasnik I, McKinney SA, Ha T. 2005. *Acc. Chem. Res.* 38:542–48
25. Myong S, Rasnik I, Joo C, Lohman TM, Ha T. 2005. *Nature* 437:1321–25
26. Myong S, Bruno MM, Pyle AM, Ha T. 2007. *Science* 317:513–16
27. Joo C, McKinney SA, Nakamura M, Rasnik I, Myong S, Ha T. 2006. *Cell* 126:515–27
28. Roy R, Kozlov AG, Lohman TM, Ha T. 2007. *J. Mol. Biol.* 369:1244–57
29. Koopmans WJ, Brehm A, Logie C, Schmidt T, van Noort J. 2007. *J. Fluoresc.* 17:785–95
30. Blanchard SC, Gonzalez RL, Kim HD, Chu S, Puglisi JD. 2004. *Nat. Struct. Mol. Biol.* 11:1008–14
31. Stone MD, Mihalusova M, O'Connor CM, Prathapam R, Collins K, Zhuang XW. 2007. *Nature* 446:458–61
32. Liu HW, Zeng Y, Landes CF, Kim YJ, Zhu Y, et al. 2007. *Proc. Natl. Acad. Sci. USA* 104:5261–67
33. Graneli A, Yeykal CC, Prasad TK, Greene EC. 2006. *Langmuir* 22:292–99
34. Groll J, Amirgoulova EV, Ameringer T, Heyes CD, Rocker C, et al. 2004. *J. Am. Chem. Soc.* 126:4234–39
35. Amirgoulova EV, Groll J, Heyes CD, Ameringer T, Rocker C, et al. 2004. *Chemphyschem* 5:552–55
36. Kerssemakers JWJ, Munteanu EL, Laan L, Noetzel TL, Janson ME, Dogterom M. 2006. *Nature* 442:709–12
37. McKinney SA, Joo C, Ha T. 2006. *Biophys. J.* 91:1941–51
38. Watkins LP, Yang H. 2005. *J. Phys. Chem. B* 109:617–28
39. Hohng S, Joo C, Ha T. 2004. *Biophys. J.* 87:1328–37
40. Clamme JP, Deniz AA. 2005. *Chemphyschem* 6:74–77
41. Friedman LJ, Chung J, Gelles J. 2006. *Biophys. J.* 91:1023–31
42. Heilemann M, Kasper R, Tinnefeld P, Sauer M. 2006. *J. Am. Chem. Soc.* 128:16864–75
43. Ross J, Buschkamp P, Fetting D, Donnermeyer A, Roth CM, Tinnefeld P. 2007. *J. Phys. Chem. B* 111:321–26
44. Edel JB, Eid JS, Meller A. 2007. *J. Phys. Chem. B* 111:2986–90
45. Gratton E, Breusegem S, Sutin J, Ruan Q, Barry N. 2003. *J. Biomed. Opt.* 8:381–90
46. Maus M, Cotlet M, Hofkens J, Gensch T, De Schryver FC, et al. 2001. *Anal. Chem.* 73:2078–86
47. Köllner M, Wolfrum J. 1992. *Chem. Phys. Lett.* 200:199–204
48. Yang H, Luo G, Karnchanaphanurach P, Louie TM, Rech I, et al. 2003. *Science* 302:262–66
49. Deniz AA, Dahan M, Grunwell JR, Ha T, Faulhaber AE, et al. 1999. *Proc. Natl. Acad. Sci. USA* 96:3670–75
50. Schuler B, Lipman EA, Eaton WA. 2002. *Nature* 419:743–47

Annu. Rev. Biochem. 2008.77:51-76. Downloaded from www.annualreviews.org
by Kanazawa University Medical Library Branch on 09/07/10. For personal use only.

51. Deniz AA, Laurence TA, Beligere GS, Dahan M, Martin AB, et al. 2000. *Proc. Natl. Acad. Sci. USA* 97:5179–84
52. Lipman EA, Schuler B, Bakajin O, Eaton WA. 2003. *Science* 301:1233–35
53. Higuchi H, Muto E, Inoue Y, Yanagida T. 1997. *Proc. Natl. Acad. Sci. USA* 94:4395–400
54. Abbondanzieri EA, Shaevitz JW, Block SM. 2005. *Biophys. J.* 89:L61–63
55. White SS, Balasubramanian S, Klenerman D, Ying LM. 2006. *Angew. Chem. Int. Ed. Engl.* 45:7540–43
56. Diez M, Zimmermann B, Borsch M, Konig M, Schweinberger E, et al. 2004. *Nat. Struct. Mol. Biol.* 11:135–41
57. Kapanidis AN, Lee NK, Laurence TA, Doose S, Margeat E, Weiss S. 2004. *Proc. Natl. Acad. Sci. USA* 101:8936–41
58. Kapanidis AN, Margeat E, Ho SO, Kortkhonjia E, Weiss S, Ebright RH. 2006. *Science* 314:1144–47
59. Lee NK, Kapanidis AN, Wang Y, Michalet X, Mukhopadhyay J, et al. 2005. *Biophys. J.* 88:2939–53
60. Rüttinger S, Macdonald R, Krämer B, Koberling F, Roos M, Hildt E. 2006. *J. Biomed. Opt.* 11:024012
61. Laurence TA, Kong X, Jager M, Weiss S. 2005. *Proc. Natl. Acad. Sci. USA* 102:17348–53
62. Muller BK, Zaychikov E, Brauchle C, Lamb DC. 2005. *Biophys. J.* 89:3508–22
63. Margeat E, Kapanidis AN, Tinnefeld P, Wang Y, Mukhopadhyay J, et al. 2006. *Biophys. J.* 90:1419–31
64. Lee NK, Kapanidis AN, Koh HR, Korlann Y, Ho SO, et al. 2007. *Biophys. J.* 92:303–12
65. Widengren J, Kudryavtsev V, Antonik M, Berger S, Gerken M, Seidel CAM. 2006. *Anal. Chem.* 78:2039–50
66. Levene MJ, Korlach J, Turner SW, Foquet M, Craighead HG, Webb WW. 2003. *Science* 299:682–86
67. Samiee KT, Moran-Mirabal JM, Cheung YK, Craighead HG. 2006. *Biophys. J.* 90:3288–99
68. Braslavsky I, Hebert B, Kartalov E, Quake SR. 2003. *Proc. Natl. Acad. Sci. USA* 100:3960–64
69. Boukobza E, Sonnenfeld A, Haran G. 2001. *J. Phys. Chem. B* 105:12165–70
70. Rhoades E, Gussakovsky E, Haran G. 2003. *Proc. Natl. Acad. Sci. USA* 100:3197–202
71. Okumus B, Wilson TJ, Lilley DM, Ha T. 2004. *Biophys. J.* 87:2798–806
72. Cisse I, Okumus B, Joo C, Ha T. 2007. *Proc. Natl. Acad. Sci. USA* 104:12646–50
73. Cheung MS, Klimov D, Thirumalai D. 2005. *Proc. Natl. Acad. Sci. USA* 102:4753–58
74. Pielak GJ. 2005. *Proc. Natl. Acad. Sci. USA* 102:5901–2
75. English BP, Min W, van Oijen AM, Lee KT, Luo GB, et al. 2006. *Nat. Chem. Biol.* 2:87–94
76. Zhuang XW, Kim H, Pereira MJB, Babcock HP, Walter NG, Chu S. 2002. *Science* 296:1473–76
77. Schmidt T, Schutz GJ, Baumgartner W, Gruber HJ, Schindler H. 1996. *Proc. Natl. Acad. Sci. USA* 93:2926–29
78. Thompson RE, Larson DR, Webb WW. 2002. *Biophys. J.* 82:2775–83
79. Yildiz A, Forkey JN, McKinney SA, Ha T, Goldman YE, Selvin PR. 2003. *Science* 300:2061–65
80. Benesch RE, Benesch R. 1953. *Science* 118:447–48
81. Rasnik I, McKinney SA, Ha T. 2006. *Nat. Methods* 3:891–93
82. Warshaw DM, Kennedy GG, Work SS, Krementsova EB, Beck S, Trybus KM. 2005. *Biophys. J.* 88:L30–32

First work utilizing porous vesicles for the single-molecule study.

Tracked diffusing membrane proteins with the accuracy of several nanometers.

Tracked a motor protein with nanometer accuracy via single-molecule fluorescence.

83. Churchman LS, Okten Z, Rock RS, Dawson JF, Spudich JA. 2005. *Proc. Natl. Acad. Sci. USA* 102:1419–23
84. Lacoste TD, Michalet X, Pinaud F, Chemla DS, Alivisatos AP, Weiss S. 2000. *Proc. Natl. Acad. Sci. USA* 97:9461–66
85. Gordon MP, Ha T, Selvin PR. 2004. *Proc. Natl. Acad. Sci. USA* 101:6462–65
86. Qu X, Wu D, Mets L, Scherer NF. 2004. *Proc. Natl. Acad. Sci. USA* 101:11298–303
87. Balci H, Ha T, Sweeney HL, Selvin PR. 2005. *Biophys. J.* 89:413–17
88. Adachi K, Yasuda R, Noji H, Itoh H, Harada Y, et al. 2000. *Proc. Natl. Acad. Sci. USA* 97:7243–47
89. Sase I, Miyata H, Ishiwata S, Kinosita K Jr. 1997. *Proc. Natl. Acad. Sci. USA* 94:5646–50
90. Sosa H, Peterman EJ, Moerner WE, Goldstein LS. 2001. *Nat. Struct. Biol.* 8:540–44

Provided a detailed description of the rotations of F1-ATPase via polarization microscopy.

91. Nishizaka T, Oiwa K, Noji H, Kimura S, Muneyuki E, et al. 2004. *Nat. Struct. Mol. Biol.* 11:142–48

92. Sick B, Hecht B, Novotny L. 2000. *Phys. Rev. Lett.* 85:4482–85
93. Dickson RM, Norris DJ, Moerner WE. 1998. *Phys. Rev. Lett.* 81:5322–25
94. Toprak E, Enderlein J, Syed S, McKinney SA, Petschek RG, et al. 2006. *Proc. Natl. Acad. Sci. USA* 103:6495–99
95. Xie XS, Yu J, Yang WY. 2006. *Science* 312:228–30
96. Harms GS, Cognet L, Lommerse PHM, Blab GA, Schmidt T. 2001. *Biophys. J.* 80:2396–408
97. Sako Y, Yanagida T. 2003. *Nat. Rev. Mol. Cell Biol.* Sept. (Suppl.):SS1–5
98. Iino R, Koyama I, Kusumi A. 2001. *Biophys. J.* 80:2667–77
99. Harms GS, Cognet L, Lommerse PHM, Blab GA, Kahr H, et al. 2001. *Biophys. J.* 81:2639–46
100. Murakoshi H, Iino R, Kobayashi T, Fujiwara T, Ohshima C, et al. 2004. *Proc. Natl. Acad. Sci. USA* 101:7317–22
101. Lommerse PHM, Blab GA, Cognet L, Harms GS, Snaar-Jagalska BE, et al. 2004. *Biophys. J.* 86:609–16
102. Douglass AD, Vale RD. 2005. *Cell* 121:937–50
103. Ulbrich MH, Isacoff EY. 2007. *Nat. Methods* 4:319–21
104. Sako Y, Minoghchi S, Yanagida T. 2000. *Nat. Cell Biol.* 2:168–72
105. Ueda M, Sako Y, Tanaka T, Devreotes P, Yanagida T. 2001. *Science* 294:864–67
106. Vrljic M, Nishimura SY, Brasselet S, Moerner WE, McConnell HM. 2002. *Biophys. J.* 83:2681–92
107. Dahan M, Levi S, Luccardini C, Rostaing P, Riveau B, Triller A. 2003. *Science* 302:442–45

First observation of protein translation at the single-molecule level in a live cell.

108. Yu J, Xiao J, Ren XJ, Lao KQ, Xie XS. 2006. *Science* 311:1600–3

109. Elf J, Li GW, Xie XS. 2007. *Science* 316:1191–94
110. Yang W, Gelles J, Musser SM. 2004. *Proc. Natl. Acad. Sci. USA* 101:12887–92
111. Kural C, Kim H, Syed S, Goshima G, Gelfand VI, Selvin PR. 2005. *Science* 308:1469–72
112. Nan XL, Sims PA, Chen P, Xie XS. 2005. *J. Phys. Chem. B* 109:24220–24
113. Leduc C, Ruhnow F, Howard J, Diez S. 2007. *Proc. Natl. Acad. Sci. USA* 104:10847–52
114. Bertrand E, Chartrand P, Schaefer M, Shenoy SM, Singer RH, Long RM. 1998. *Mol. Cell* 2:437–45

Annu. Rev. Biochem. 2008.77:51-76. Downloaded from www.annualreviews.org
by Kanazawa University Medical Library Branch on 09/07/10. For personal use only.

115. Fusco D, Accornero N, Lavoie B, Shenoy SM, Blanchard JM, et al. 2003. *Curr. Biol.* 13:161–67
116. Golding I, Cox EC. 2004. *Proc. Natl. Acad. Sci. USA* 101:11310–15
117. Golding I, Paulsson J, Zawilski SM, Cox EC. 2005. *Cell* 123:1025–36
118. Chubb JR, Trcek T, Shenoy SM, Singer RH. 2006. *Curr. Biol.* 16:1018–25
119. Seisenberger G, Ried MU, Endress T, Buning H, Hallek M, Brauchle C. 2001. *Science* 294:1929–32
120. Lakadamyali M, Rust MJ, Babcock HP, Zhuang XW. 2003. *Proc. Natl. Acad. Sci. USA* 100:9280–85
121. Lakadamyali M, Rust MJ, Zhuang XW. 2006. *Cell* 124:997–1009
122. Ishijima A, Kojima H, Funatsu T, Tokunaga M, Higuchi H, et al. 1998. *Cell* 92:161–71
123. Lang MJ, Fordyce PM, Block SM. 2003. *J. Biol.* 2:6
124. Brau RR, Tarsa PB, Ferrer JM, Lee P, Lang MJ. 2006. *Biophys. J.* 91:1069–77
125. Tarsa PB, Brau RR, Barch M, Ferrer JM, Freyzon Y, et al. 2007. *Angew. Chem. Int. Ed. Engl.* 46:1999–2001
126. Hohng S, Zhou R, Nahas MK, Yu J, Schulten K, et al. 2007. *Science* 318:279–83
127. Uemura S, Dorywalska M, Lee TH, Kim HD, Puglisi JD, Chu S. 2007. *Nature* 446:454–57
128. Shroff H, Reinhard BM, Siu M, Agarwal H, Spakowitz A, Liphardt J. 2005. *Nano Lett.* 5:1509–14
129. Hugel T, Michaelis J, Hetherington CL, Jardine PJ, Grimes S, et al. 2007. *PLoS Biol.* 5:e59
130. Strick TR, Allemand JF, Bensimon D, Bensimon A, Croquette V. 1996. *Science* 271:1835–37
131. Graneli A, Yeykal CC, Robertson RB, Greene EC. 2006. *Proc. Natl. Acad. Sci. USA* 103:1221–26
132. Blainey PC, van Oijen AM, Banerjee A, Verdine GL, Xie XS. 2006. *Proc. Natl. Acad. Sci. USA* 103:5752–57
133. Amitani I, Baskin RJ, Kowalczykowski SC. 2006. *Mol. Cell* 23:143–48
134. Prasad TK, Robertson RB, Visnapuu ML, Chi P, Sung P, Greene EC. 2007. *J. Mol. Biol.* 369:940–53
135. Greene EC, Mizuuchi K. 2002. *Mol. Cell* 9:1079–89
136. Galletto R, Amitani I, Baskin RJ, Kowalczykowski SC. 2006. *Nature* 443:875–78
137. Song L, Varma CA, Verhoeven JW, Tanke HJ. 1996. *Biophys. J.* 70:2959–68
138. Hoebe RA, Van Oven CH, Gadella TW Jr, Dhonukshe PB, Van Noorden CJF, Manders EM. 2007. *Nat. Biotechnol.* 25:249–53
139. Eggeling C, Widengren J, Brand L, Schaffer J, Felekyan S, Seidel CAM. 2006. *J. Phys. Chem. A* 110:2979–95
140. Kong X, Nir E, Hamadani K, Weiss S. 2007. *J. Am. Chem. Soc.* 129:4643–54
141. Donnert G, Eggeling C, Hell SW. 2007. *Nat. Methods* 4:81–86
142. Köhn F, Hofkens J, Gronheid R, Van der Auweraer M, De Schryver FC. 2002. *J. Phys. Chem. A* 106:4808–14
143. Widengren J, Schwille P. 2000. *J. Phys. Chem. A* 104:6416–28
144. Sabanayagam CR, Eid JS, Meller A. 2005. *J. Chem. Phys.* 123:224708
145. Michalet X, Pinaud FF, Bentolila LA, Tsay JM, Doose S, et al. 2005. *Science* 307:538–44
146. Medintz IL, Uyeda HT, Goldman ER, Mattoussi H. 2005. *Nat. Mater.* 4:435–46

Annu. Rev. Biochem. 2008.77:51-76. Downloaded from www.annualreviews.org
by Kanazawa University Medical Library Branch on 09/07/10. For personal use only.

147. Hohng S, Ha T. 2005. *Chemphyschem* 6:956–60
148. Hohng S, Ha T. 2004. *J. Am. Chem. Soc.* 126:1324–25
149. Syed S, Snyder GE, Franzini-Armstrong C, Selvin PR, Goldman YE. 2006. *EMBO J.* 25:1795–803

RELATED RESOURCES

Selvin PR, Ha T, eds. 2008. *Single Molecule Techniques: A Laboratory Manual.* Cold Spring Harbor, NY: Cold Spring Harb. Lab. 1st ed.
Lakowicz JR. 2006. *Principles of Fluorescence Spectroscopy*. Berlin: Springer, 3rd ed.
Toprak E, Selvin PR. 2007. *Annu. Rev. Biophys. Biomol. Struct.* 36:349–69
Rosenberg SA, Quinlan ME, Forkey JN, Goldman YE. 2005. *Acc. Chem. Res.* 38:583–93

Annu. Rev. Biochem. 2008.77:51-76. Downloaded from www.annualreviews.org
by Kanazawa University Medical Library Branch on 09/07/10. For personal use only.

Annual Review of Biochemistry

Volume 77, 2008

Contents

Annu. Rev. Biochem. 2008.77:51-76. Downloaded from www.annualreviews.org
by Kanazawa University Medical Library Branch on 09/07/10. For personal use only.

Prefatory Chapters

Discovery of G Protein Signaling
Zvi Selinger 1

Moments of Discovery
Paul Berg 14

Single-Molecule Theme

In singulo Biochemistry: When Less Is More
Carlos Bustamante 45

Advances in Single-Molecule Fluorescence Methods for Molecular Biology
Chirlmin Joo, Hamza Balci, Yuji Ishitsuka, Chittanon Buranachai, and Taekjip Ha 51

How RNA Unfolds and Refolds
Pan T.X. Li, Jeffrey Vieregg, and Ignacio Tinoco, Jr. 77

Single-Molecule Studies of Protein Folding
Alessandro Borgia, Philip M. Williams, and Jane Clarke 101

Structure and Mechanics of Membrane Proteins
Andreas Engel and Hermann E. Gaub 127

Single-Molecule Studies of RNA Polymerase: Motoring Along
Kristina M. Herbert, William J. Greenleaf, and Steven M. Block 149

Translation at the Single-Molecule Level
R. Andrew Marshall, Colin Echeverría Aitken, Magdalena Dorywalska, and Joseph D. Puglisi 177

Recent Advances in Optical Tweezers
Jeffrey R. Moffitt, Yann R. Chemla, Steven B. Smith, and Carlos Bustamante 205

Recent Advances in Biochemistry

Mechanism of Eukaryotic Homologous Recombination
Joseph San Filippo, Patrick Sung, and Hannah Klein 229

Structural and Functional Relationships of the XPF/MUS81 Family of Proteins
Alberto Ciccia, Neil McDonald, and Stephen C. West 259

Fat and Beyond: The Diverse Biology of PPARγ
Peter Tontonoz and Bruce M. Spiegelman 289

Eukaryotic DNA Ligases: Structural and Functional Insights
Tom Ellenberger and Alan E. Tomkinson 313

Structure and Energetics of the Hydrogen-Bonded Backbone in Protein Folding
D. Wayne Bolen and George D. Rose 339

Macromolecular Modeling with Rosetta
Rhiju Das and David Baker 363

Activity-Based Protein Profiling: From Enzyme Chemistry to Proteomic Chemistry
Benjamin F. Cravatt, Aaron T. Wright, and John W. Kozarich 383

Analyzing Protein Interaction Networks Using Structural Information
Christina Kiel, Pedro Beltrao, and Luis Serrano 415

Integrating Diverse Data for Structure Determination of Macromolecular Assemblies
Frank Alber, Friedrich Förster, Dmitry Korkin, Maya Topf, and Andrej Sali 443

From the Determination of Complex Reaction Mechanisms to Systems Biology
John Ross 479

Biochemistry and Physiology of Mammalian Secreted Phospholipases A_2
Gérard Lambeau and Michael H. Gelb 495

Glycosyltransferases: Structures, Functions, and Mechanisms
L.L. Lairson, B. Henrissat, G.J. Davies, and S.G. Withers 521

Structural Biology of the Tumor Suppressor p53
Andreas C. Joerger and Alan R. Fersht 557

Toward a Biomechanical Understanding of Whole Bacterial Cells
Dylan M. Morris and Grant J. Jensen 583

How Does Synaptotagmin Trigger Neurotransmitter Release?
Edwin R. Chapman 615

Protein Translocation Across the Bacterial Cytoplasmic Membrane
Arnold J.M. Driessen and Nico Nouwen 643

Annu. Rev. Biochem. 2008.77:51-76. Downloaded from www.annualreviews.org
by Kanazawa University Medical Library Branch on 09/07/10. For personal use only.

Maturation of Iron-Sulfur Proteins in Eukaryotes: Mechanisms, Connected Processes, and Diseases
Roland Lill and Ulrich Mühlenhoff 669

CFTR Function and Prospects for Therapy
John R. Riordan 701

Aging and Survival: The Genetics of Life Span Extension by Dietary Restriction
William Mair and Andrew Dillin 727

Cellular Defenses against Superoxide and Hydrogen Peroxide
James A. Imlay 755

Toward a Control Theory Analysis of Aging
Michael P. Murphy and Linda Partridge 777

Indexes

Cumulative Index of Contributing Authors, Volumes 73–77 799

Cumulative Index of Chapter Titles, Volumes 73–77 803

Errata

An online log of corrections to *Annual Review of Biochemistry* articles may be found at http://biochem.annualreviews.org/errata.shtml

Annu. Rev. Biochem. 2008.77:51-76. Downloaded from www.annualreviews.org
by Kanazawa University Medical Library Branch on 09/07/10. For personal use only.